# A direct interaction between fascin and microtubules contributes to adhesion dynamics and cell migration

Giulia Villari[1,5], Asier Jayo[1,5], Jennifer Zanet[1,2], Briana Fitch[1,7], Bryan Serrels[3], Margaret Frame[3], Brian M. Stramer[1], Benjamin T. Goult[4], Maddy Parsons[1, 6]

[1] Randall Division of Cell and Molecular Biophysics, King's College London, Guys Campus, London SE1 1UL, UK

[2] Université de Toulouse, Université Paul Sabatier and Centre National de la Recherche Scientifique, Unité Mixte de Recherche 5547, Centre de Biologie du Développement, F-31062 Toulouse, France

[3] Edinburgh Cancer Research UK Centre, Institute of Genetics and Molecular Medicine, University of Edinburgh, Western General Hospital, Edinburgh EH4 2XR

[4] School of Biosciences, University of Kent, Canterbury, Kent, CT2 7NJ

[5] These authors contributed equally to this study

[6] Corresponding author: email maddy.parsons@kcl.ac.uk. Tel: +44 2078488164; Fax +44 2078486435

[7] Current address: BMS Graduate program, UCSF, 513 Parnassus Ave, San Francisco, CA 94143-0505, USA

**Keywords**: Fascin; cytoskeleton; actin; microtubule; focal adhesion; migration; focal adhesion kinase



**JCS Advance Online Article. Posted on 5 November 2015**

**Abstract:**

Fascin is an actin-binding and bundling protein that is highly upregulated in most epithelial cancers. Fascin promotes cell migration and adhesion dynamics in vitro and tumour cell metastasis in vivo. However, potential non-actin bundling roles for fascin remain unknown. Here we show for the first time that fascin can directly interact with the microtubule cytoskeleton and that this does not depend upon fascin-actin bundling. Microtubule binding contributes to fascin-dependent control of focal adhesion dynamics and cell migration speed. We also show that fascin forms a complex with focal adhesion kinase (FAK) and Src, and that this signalling pathway lies downstream of fascin-microtubule association in the control of adhesion stability. These findings shed light on new non actin-dependent roles for fascin and may have implications for the design of therapies to target fascin in metastatic disease.

**Introduction:**

Fascin is a highly conserved, 55kDa actin-binding and bundling protein that is required for the maintenance and stability of parallel bundles of filamentous (F-) actin in a variety of cellular contexts (Jayo and Parsons, 2010). Fascin is highly upregulated in most invasive cancers and is increasingly recognized as a prognostic marker of metastatic disease and has thus received considerable recent attention as a potential therapeutic target (Bi et al., 2012; Gao et al., 2012; Hashimoto et al., 2006; Jayo and Parsons, 2010; Li et al., 2008). Actin bundling occurs through two sites in fascin at the N- and C-terminus of the protein. The best characterized of these sites lies between aa33-47, through which actin binding is negatively controlled by protein kinase C (PKC)-dependent phosphorylation on serine39. Modification of this site has also been shown to play a role in association between fascin and p75NTR, Rab35 and LIM-Kinase, the latter of which supports fascin-dependent filopodia stabilization (Jayo et al., 2012; Shonukan et al., 2003; Zhang et al., 2009). Previous structural studies have proposed a second actin-binding domain between aa277-493, but how this site is regulated is not yet understood (Ono et al., 1997a).

Fascin-actin binding has been shown to play a central role in the regulation of adhesion, migration and invasion in a range of cell types and contexts (Jayo and Parsons, 2010). Most of these functions have been attributed to fascin-dependent effects on filopodia stabilization and that ultimately impact upon efficient directed migration and invasion. We have previously shown that depletion of fascin results in significantly reduced focal adhesion (FA) dynamics (Hashimoto et al., 2007) and recent work has shown this partially requires the canonical actin-bundling function of fascin to modulate cell contractility (Elkhatib et al., 2014). Dynamic focal adhesions are known to be under the control of both actin and microtubule (MT) cytoskeletons; F-actin stress fibres provide an anchor for FA stability and growth, whereas MT have been shown to target adhesion sites and mediate disassembly (Ciobanasu et al., 2013; Etienne-Manneville, 2013). We have recently shown that phosphorylation of serine274 (S289 in *Drosophila)* within the second actin-binding site also plays a key role in controlling fascin-actin bundling and filopodia assembly in vitro and in vivo (Zanet et al., 2012a). However, fascin mutated at S274 is able to support cell motility independently of actin-bundling, suggesting that other currently unknown binding partners or functions exist for this molecule that contribute to cell adhesion and migration (Zanet et al., 2012a).

In the present study, we set out to test the hypothesis that fascin has non-actin bundling dependent binding partners that contribute to cell adhesion and migration. Our results provide evidence of a novel interaction between fascin and the MT cytoskeleton and show that this association does not require fascin-actin bundling. Loss of fascin results in more stable microtubules in cells and in vivo, and blocking fascin-MT binding leads to more stable adhesions and slower cell migration. We further show that dynamic MT promote the formation of a complex between fascin, focal adhesion kinase (FAK) and Src. Expression of MT-binding mutants of fascin leads to more stable adhesions, and this phenotype can be reversed by

overexpressing constitutively active Src, contributing to FA disassembly. Thus our data show a novel role for fascin in control of migration through associating with microtubules. This has broader implications for understanding fascin in other biological contexts as well as in the design of therapeutic agents to inhibit metastatic disease.

**Results**

***Depletion of fascin results in larger focal adhesions and less dynamic microtubules***

To analyse the role of fascin in controlling FA assembly we generated MDA MB 231 and HeLa human cancer cell lines stably expressing shRNA to efficiently deplete endogenous fascin (fasKD) followed by expression of wild-type fascin-GFP (resWT; Fig S1A). Analysis of fixed cells stained for phosphotyrosine (p-Tyr) as focal adhesion marker demonstrated that knockdown of fascin increased the percentage of MDA MB 231 cell area occupied by focal adhesions compared to control or resWT cells (Fig 1A), but with no change in total adhesion protein levels (Fig S1B) or spread cell area (not shown). We also saw similar changes in focal adhesion coverage in HeLa cells depleted of fascin (Fig S1C), which is consistent with our own previous observations (Hashimoto et al., 2007) and a more recent report in colon carcinoma cells (Elkhatib et al., 2014). This finding was further confirmed in mouse NIH3T3 fibroblasts that also express high levels of endogenous fascin suggesting that this role for fascin also extends to non-tumour cells (Fig S1D). To enable quantitative analysis of focal adhesion disassembly in a synchronised manner, we performed Nocodazole (NOC) washout assays in control, fascin knockdown and resWT cells. NOC induces MT depolymerisation and treatment of cells with this drug has previously been shown to result in FA growth followed by rapid adhesion disassembly upon drug washout (Ezratty et al., 2005). Analysis of adhesions in fascin depleted or rescued MDA MB 231 cells demonstrated a significant reduction in dynamic focal adhesion growth and disassembly upon NOC treatment upon fascin knockdown (Fig 1B, 1C). We further confirmed this defective focal adhesion disassembly upon microtubule disruption in fixed HeLa and NIH 3T3 cells (Fig S1C and D respectively). Live cell time-lapse confocal imaging also demonstrated a significantly reduced adhesion disassembly response to Nocodazole washout in fascin-depleted MDA MB 231 cells expressing vinculin-mRFP (Fig S1E). These data combined suggest that fascin is required for regulated microtubule-dependent focal adhesion dynamics in both tumour-derived and non-cancer cell types.

To determine whether loss of fascin had an impact on MT growth, we fixed control, fascin knockdown and resWT cells throughout the NOC washout assay and stained these cells for tubulin. Images of these cells revealed that loss of fascin led to a significant delay in MT re-growth following NOC washout as compared to control cells (Fig 1D). F-actin staining also demonstrated that fascin knockdown cells retained thicker stress fibres at 60 minutes washout in agreement with previous observations in fascin depleted colon carcinoma cells (Elkhatib et al., 2014). To investigate whether the observed defects in fascin silenced cells were due to effects on MT dynamics, we performed time-lapse imaging of tubulin-mCherry expressing

control or fascinKD HeLa cells under basal conditions. HeLa cells represent an excellent and well characterised model cell line to study MT dynamics as they have a large cytoplasmic spread surface area to study individual MTs by fluorescence time-lapse microscopy. Analysis of individual microtubule behaviour over time (Fig 1E for snapshots and Supplementary Movie1) revealed that depleting fascin resulted in significantly more stable MT exhibiting slower growth and fewer catastrophe events compared to MT in control shRNA cells (quantification in Fig1F) in agreement with the analysis of MT re-growth following NOC washout. Western blotting further demonstrated that acetylated tubulin, a marker of stable MT (Webster and Borisy, 1989), was increased in fascin-silenced cells (Fig S2A). These data combined demonstrate that fascin contributes to the dynamics and stability of microtubules.

We next wanted to determine whether fascin plays a role in MT stability *in vivo*. We have previously shown that fascin is required for cell migration in haemocyte blood cells within the developing *Drosophila* embryo, where it can stabilize F-actin bundles at the leading edge (Zanet et al., 2012a; Zanet et al., 2009). In order to determine whether fascin could also co-operate with MT within an *in vivo* setting, we imaged fascin-mCherry and the MT +TIP protein CLIP-GFP in migrating haemocytes in developing *Drosophila* embryos. Images demonstrated that partial colocalisation between fascin and MT bundles occurred within the lamellae, and these MT bundles have previously been shown to be required for directed migration in these cells (Fig 1G; (Stramer et al., 2010)). As our data in human and mouse cells demonstrated a role for fascin in promoting dynamic MTs, we analysed the growth phase time of MT bundles that colocalised with fascin compared to non-fascin associated bundles in the same migrating haemocyte and cumulated this data from multiple different cells and embryos for analysis. Data showed a significant increase in the MT growth phase time in non-fascin associated bundles (Fig 1G, Supplementary Movie 2), in agreement with analysis in fascin-depleted human cancer cells. Taken together these data support a novel and conserved role for fascin in the regulation of MT stability both *in vitro* and *in vivo*.

***Fascin associates directly with microtubules in vitro and in cells***

One possible explanation for the observed fascin-dependent defects in MT dynamics is a direct or indirect association of fascin with the MT network. To first explore the possibility of a direct interaction, we performed *in vitro* co-sedimentation assays between *in vitro* purified fascin and polymerised, taxol stabilised purified tubulin. In the absence of tubulin, fascin was not detectable in the high-speed pellet; however ~25% of fascin, but not a BSA protein control, was observed to co-sediment in the high-speed fraction when combined with Taxol-stabilised MT (Fig 2A), suggesting that fascin and MT may directly interact. We next sought to identify a potential binding domain for MT within the sequence of fascin. Although MT-binding domains are diverse in sequence and charge, recent bioinformatics approaches have proposed some common features in these domains across different MT binding protein classes (Cao and Mao, 2009). Inspection of the fascin protein sequence revealed a basic, lysine-rich putative MT-binding

sequence within the C-terminal region of the second β-trefoil domain (aa234-250; Fig 2B). To further investigate whether this domain may play a role in fascin-MT binding, we generated purified fascin protein mutated at five residues within this region (S/S/T/K/K>A; herein referred to as MT1) or lacking this 16 amino acid stretch (herein referred to as ΔMT1) and performed MT co-sedimentation assay analysis as before. Previous studies have demonstrated that mutating regions within MT-binding domains to Alanine in other MT-binding proteins such as kinesin and doublecortin results in more stable association (Klumpp et al., 2003; Makrantoni et al., 2014; Schaar et al., 2004; Zhu et al., 2010). Consistent with these studies, purified mutant MT1-fascin showed significantly higher association with polymerized MT compared to WT fascin protein, whereas ΔMT1-fascin association with the MT pellet was significantly lower (Fig 2C). These data combined demonstrate that fascin can directly bind to polymerised microtubules *in vitro*, and that aa234-250 may act as a stabilizing interface in this association.

To confirm that the direct interaction between fascin and MT also occurred in the context of an intact cell, we performed fluorescence lifetime imaging microscopy (FLIM) to analyse fluorescence resonance energy transfer (FRET) between GFP-fascin and tubulin-mCherry (as we have previously for fascin-F-actin binding (Jayo et al., 2012; Zanet et al., 2012a)). Fluorescence lifetime maps of individual cells and cumulative FRET efficiency analysis both revealed a direct association between WTfascin and MT (Fig 2D). In agreement with our *in vitro* data, ΔMT1-fascin showed significantly reduced FRET with tubulin in cells, whereas MT1-fascin showed significantly higher association with MT under the same conditions (Fig 2D). Tubulin-GFP and mCherry-WTfascin exhibited similar levels of FRET, whereas GFP-fascin co-expressed with mCherry alone showed no FRET demonstrating binding was not non-specific or dependent upon the fluorophore pairs used (data not shown). Phenotypic analysis revealed that MT re-growth following NOC washout occurred efficiently in fascin depleted cells re-expressing GFP-WT or MT1-fascin, but was significantly delayed in ΔMT1-fascin expressing cells again supporting a role for fascin binding to tubulin in controlling MT dynamics (Fig 2E). Moreover, analysis of MT dynamics in cells co-expressing WT, ΔMT1 or MT1 fascin-GFP and tubulin-mCherry revealed a reduced MT growth rate in ΔMT1 fascin cells and a significant reduction in catastrophe events in cells expressing MT1 fascin (Fig 2F and Supplementary Movie 3). Thus we conclude that fascin and MT are able to form a direct complex both *in vitro* and *in vivo* and that this association plays a role in controlling MT dynamics.

***Fascin-MT binding occurs independently of fascin-actin binding***

To determine whether the aa234-250 region also contributed to fascin-actin binding, purified MT1- and ΔMT1-fascin were assessed for their ability to bundle fluorescent F-actin using co-sedimentation assays followed by confocal microscopy. Images of *in vitro* polymerised Alexa-488 labelled F-actin showed that MT1-fascin was unable to support bundling to levels seen with the WT fascin protein, however F-actin bundles were still visible in the preparation containing ΔMT1 (Fig S2B). Similarly, when the same assay was

performed and analysed biochemically, ΔMT1- and WT fascin were able to co-sediment with F-actin to a similar degree *in vitro*, whereas MT1-fascin showed a significant reduction in pelleting (Fig S2C). Moreover, FLIM analysis of FRET between fascin and F-actin demonstrated a similar association between ΔMT1fascin and F-actin compared to WT fascin, (Fig S2D) further supporting our in vitro evidence that aa234-250 in fascin are not required for F-actin binding. These data demonstrate that disrupting fascin-MT binding does not interfere with fascin-F-actin binding *in vitro*. To further determine whether fascin MT1 or ΔMT1 mutants altered cytoskeletal assembly in cells, we expressed GFP-tagged forms of fascin mutants in fascinKD cells and analysed F-actin organization compared to control cells. In agreement with the in vitro analysis, fascinKD cells re-expressing MT1-fascin that binds more stably to MT did not exhibit restored filopodia formation compared to WT fascin rescued cells (Fig 2G). However, a partial rescue of filopodia assembly was seen in cells expressing ΔMT1-fascin compared to fascinKD cells demonstrating that non-microtubule binding mutants of fascin are still able to support F-actin bundling (Fig 2G). The partial rescue of filopodia assembly in the cells expressing the non-MT associated fascin is still functional and able to position at the cell periphery in order to associate with and bundle F-actin. Together these data demonstrate that fascin-actin bundling can occur when fascin-MT binding is disrupted, suggesting the two events are independent of one another and potentially mutually exclusive.

***Fascin-dependent focal adhesion assembly requires fascin-MT binding***

We next asked whether the direct interaction between fascin and MT functionally contributed to adhesion dynamics. To this end, adhesion disassembly following nocodazole washout was quantified in fascinKD cells re-expressing WT, MT1 or ΔMT1 fascin-GFP as in Figure1. Cells expressing MT1 or ΔMT1 fascin mutants were both unable to rescue adhesion dynamics following NOC washout to levels seen in WTfascin expressing cells (Fig 2H). ΔMT1 fascin cells failed to disassemble adhesions following NOC washout, in agreement with the lack of MT recovery in these cells at the same time point (Fig2E). Surprisingly however, MT1 fascin-expressing cells showed a significant increase in adhesion size following NOC washout (Fig 2H) suggesting that stabilising the fascin-MT complex also results in more stable focal adhesions. We postulated that the reduced focal adhesion dynamics in these cells might correlate with altered microtubule stability. In support of this, analysis of acetylated tubulin levels by western blot under basal conditions demonstrated higher levels in ΔMT1 fascin expressing cells and less stable MT in MT1 fascin cells in both HeLa and MDA MB 231 cells (Fig 2I and data not shown). This data combined demonstrates that fascin-MT binding plays a role in MT stability and that this contributes to focal adhesion disassembly.

***Fascin-dependent cell migration requires both microtubule and F-actin binding***

Our data has demonstrated that fascin can associate with MT directly, and that binding to MT and F-actin may occur in a mutually exclusive manner. We therefore next asked whether the known sites in fascin that control actin-binding might also contribute to the formation of the fascin-MT complex. To determine this,

we repeated the microtubule co-sedimentation assays with purified WT fascin or previously characterized mutants of fascin to mimic phospho (S>D) or non-phospho (S>A) states at S39 or S274 (Zanet et al., 2012a). S39D, S274A and S274D are all unable to bundle F-actin as efficiently as WT fascin, whereas S39A fascin forms highly stable F-actin bundles *in vitro* and in cells (Ono et al., 1997b; Vignjevic et al., 2006; Zanet et al., 2012a). All fascin mutant proteins showed a degree of co-sedimentation with microtubules (Fig 3A); however, S274D fascin showed significantly higher binding compared to WT protein and other mutants (Fig 3A), as was also observed for the MT1 fascin mutant (Fig 2C). To further confirm that S274D fascin was more strongly associated with MT in cells we performed FRET/FLIM analysis between fascin and tubulin in cells as described in Fig 2D. FRET efficiency data from multiple cells demonstrated a direct interaction between fascin S274D-GFP and tubulin-mCherry that was significantly higher than both WTfascin and S39D fascin (Fig 3B). This data again supports the notion that F-actin binding mutants of fascin do not also lead to impaired fascin-microtubule association, suggesting the two cytoskeletal binding events can be independently controlled.

We next tested whether the increased binding observed between S274Dfascin and microtubules may impact on MT dynamics in cells. To determine whether actin-binding mutants of fascin could regulate MT growth in cells, we re-expressed GFP-WT or mutant fascin proteins into MDA MB 231 cells depleted of endogenous fascin. Analysis of MT re-growth following NOC washout revealed that of the four single-site mutants tested, only S274D fascin was able to support MT network re-growth in cells as efficiently as WT fascin (Fig 3C). To allow us to analyse potential crosstalk or redundancy between the two known actin-binding sites in this context, we generated double mutants (S39A/S274D and S39D/S274D) re-expressed in fascin-depleted cells. Both double mutants resulted in significantly impaired filopodia formation when expressed in fascin depleted MDA MB 231 cells, demonstrating that disrupting contact between F-actin at S274 site was sufficient to suppress F-actin bundling activity (Fig S3A). Interestingly however, expression of S39D/S274D, but not S39A/S274D fascin supported efficient MT re-growth following NOC washout (Fig 3C). This suggests that F-actin binding via the N-terminal binding domain of fascin suppresses fascin-dependent microtubule assembly. This MT growth phenotype was further confirmed by live imaging of MT dynamics in fascinKD HeLa cells co-expressing GFP-fascin variants and tubulin-mCherry. Quantification of movies and resulting data demonstrated a significant reduction in MT growth rate in cells expressing S39A fascin compared to other fascin forms, and a significant reduction in catastrophe events in S274D expressing cells (Fig 3D and Supplementary movie 4) in agreement with our analysis in fixed cells. Similarly, we also observed that expression of S289D fascin in fascin-null Drosophila haemocytes (equivalent to S274D, (Zanet et al., 2012a)) resulted in assembly of stable fascin-MT bundles and reduced MT dynamics *in vivo* compared to WT fascin (Supplementary movies 5 and 6). Collectively these data demonstrate that S274 within the C-terminal actin-binding site of fascin plays an important role in the regulation of fascin-dependent microtubule dynamics both *in vitro* and *in vivo*.

To determine whether these MT-binding differences resulted in adhesion area changes, we quantified adhesion area in cells expressing S39A, S39D, S274A or S274D mutants of fascin. Data demonstrated that S39A, S39D and S274A mutants of fascin were able to support adhesion disassembly in response to NOC washout (Fig 4A; Fig S3B). Conversely, cells expressing S274D fascin showed larger adhesions under both basal conditions and upon nocodazole washout (Fig 4A), mimicking the effect seen in cells expressing the MT1 fascin mutant, that also similarly exhibits increased MT binding (Fig 2). There were no changes in total adhesion protein levels in cells expressing fascin mutants (Fig S3C). In agreement with the MT re-growth assay data, the adhesion disassembly defect in S274D cells was partially reversed in the S39A/S274D double mutant cells, but not in the S39D/S274D cells (Fig 4A). These data together further suggest that S274 plays an important role in fascin-MT association and focal adhesion dynamics, potentially through disconnecting fascin from F-actin and promoting direct fascin-MT binding.

In order to determine whether the defects in adhesion dynamics correlated with defective cell migration, we performed phase contrast time-lapse microscopy of fascinKD cells rescued with WT or mutant fascin proteins followed by single cell tracking and analysis. Quantitative comparisons of migration tracks demonstrated that cells expressing ΔMT1 fascin or S39D fascin had slower migration speeds compared to cells rescued with WT protein (Fig 4B and 4C), suggesting loss of F-actin or MT binding is sufficient to impair fascin-dependent migration. Similarly, cells expressing MT1, S274D or S39A/S274D mutants of fascin that did not undergo efficient adhesion disassembly also showed significantly reduced migration speeds (Fig 4B and 4C). These experiments provide correlative evidence that co-ordinated control of phosphorylation at S39 and S274 residues is required for fascin-dependent microtubule assembly, adhesion disassembly and cell migration.

***Fascin regulates activation of focal adhesion kinase***

We next asked how fascin-MT binding might mechanistically impact on focal adhesion signalling. Focal adhesion kinase (FAK) is a key component of focal adhesions and is known to recruit the non-receptor tyrosine kinase Src following auto-phosphorylation at Tyr397. The activation of FAK and induction of the FAK-Src complex has previously been shown to play a key role in adhesion dynamics through clathrin-dependent endocytosis of integrins and other adhesion components (Ezratty et al., 2009; Ezratty et al., 2005; Wang et al., 2011). Furthermore, MT-induced disassembly of adhesions requires activation of the FAK-Src pathway, and disruption of the FAK phosphorylation cycle leads to enhanced FA growth and stability (Hamadi et al., 2005; Wang et al., 2011). Thus we postulated that fascin may operate upstream of the FAK-Src pathway to regulate adhesion dynamics. In order to determine whether fascin may regulate FA dynamics through this pathway, we quantified active FAK levels in lysates from control or fascinKD cells throughout the nocodazole washout assay. Data demonstrated that fascin depleted cells exhibited

significantly lower active FAK under basal conditions and also failed to activate FAK (through phosphorylation of Y397) during drug washout and FA disassembly at 60 minutes (Fig 5A). Confocal imaging and linescan analysis of WT fascin expressing cells further revealed that a population of endogenous fascin was seen colocalising with FAK and microtubules at peripheral focal adhesion sites following NOC washout (Fig 5B). Investigation of FAK and tubulin in fascin mutant expressing cells further revealed larger MT bundles overlapping with FAK-positive adhesions in S274D fascin expressing cells, and partial colocalisation between S39Afascin and FAK but not the other fascin mutants (Fig 5C). Moreover, biochemical analysis of pYFAK levels following nocodazole washout in these cells demonstrated that re-expression of S274D fascin did not support activation of FAK upon MT re-growth to the extent seen in cells expressing all other fascin forms (Fig 5D). These data together suggest that fascin is required for activation of FAK during MT-induced adhesion disassembly, and that co-ordination between these functions likely requires a dynamic cycle between fascin-actin and fascin-MT binding.

Given the partial colocalisation between fascin, FAK and microtubules we postulated that these proteins may be able to form a complex and that this complex may be dependent upon microtubule stability. To test this hypothesis, endogenous FAK was immunoprecipitated from fascinKD cells expressing WT fascin-GFP under basal conditions or following treatment with nocodazole or Taxol to disrupt or stabilise microtubules respectively. Western blotting demonstrated that fascin was readily detectable in a complex with FAK and tubulin, and that this was reduced under both conditions that disrupted MT dynamics (Fig 5E). Moreover, the FAK that was found in a complex with fascin and tubulin under basal conditions was phosphorylated at Y397, but this activation was significantly reduced in cells treated with Nocodazole or Taxol (Fig 5E). To further determine whether this complex was the result of a direct interaction between fascin and FAK, we performed pulldown experiments using purified fascin co-incubated with C-terminal or FERM domains of FAK tagged to GST. However, fascin did not bind to any FAK domain tested under these conditions suggesting these proteins do not directly interact *in vitro* (data not shown).

***Fascin-microtubule binding acts upstream of FAK and Src to regulate adhesion dynamics***

To determine whether FAK-fascin complex formation was regulated by fascin-MT binding, we performed FAK IP's from fasKD cells expressing WT, S39A, S274D or MT1 mutant forms of GFP-fascin. Data showed similar levels of WT and S39A fascin in complex with FAK; however, S274D and MT1 fascin mutants, that both exhibit increased MT binding, both showed significantly lower association in the complex (Fig 6A). Moreover, re-probes of these IP complexes revealed the presence of Src, which also showed lower co-association with FAK in cells expressing S274D or MT1 fascin (Fig 6A). Taken altogether these data suggest that fascin, FAK and Src are able to form a complex and that this is dependent upon both fascin-MT binding as well as the presence of a dynamic microtubule cytoskeleton.

As S274D fascin resulted in much larger FA and lower active FAK, we hypothesised that S274D fascin may prevent effective downstream signalling to Src. To address this, we first analysed basal levels of active FAK and Src in fascin depleted cells re-expressing either WT, S39A, S274D or MT1 fascin-GFP. Western blots showed no change in total levels of FAK or Src in any of the mutant fascin expressing cells (Fig 6B, Fig 5D). However, decreased activity of both FAK and Src were seen in S274D and MT1 fascin expressing cell lysates (Fig 6B) suggesting that fascin-MT binding affects activation of these key adhesion molecules and in agreement with similar findings in Nocodazole washout conditions (Fig 5D). We next wanted to determine whether Src was a key molecule downstream of fascin-MT binding in controlling focal adhesion dynamics. To determine this, we expressed WT or constitutively active Src (Y527F)-GFP in fascinKD cells rescued with WT, S39A, S274D or MT1 fascin-mRFP and analysed adhesion disassembly following nocodazole washout. In the presence of expressed WT Src-GFP, nocodazole washout resulted in adhesion disassembly in WT and S39Afascin expressing cells, but not those rescued with S274D or MT1 fascin mutants (Fig 6C and D), similar to the response seen previously in control cells. However, co-expression of Y527FSrc resulted in restoration of adhesion disassembly to comparable levels in all cells (Fig 6C and D), suggesting that constitutive activation of Src is able to over-ride the adhesion stabilizing effect of S274D and MT1 fascin mutants. Taken together these findings demonstrate that fascin association with microtubules, FAK and Src promotes activation of the FAK-Src complex and facilitates efficient microtubule-dependent focal adhesion disassembly.

**Discussion**

Fascin is well characterized as an actin-bundling protein that can regulate cell migration as well being an emerging important prognostic marker for metastatic disease (Bi et al., 2012; Gao et al., 2012; Hashimoto et al., 2006; Jayo and Parsons, 2010; Li et al., 2008). Here we demonstrate for the first time that fascin can associate directly with microtubules. We show that fascin-microtubule binding is in part controlled through a binding site within the second β-trefoil domain, and that disrupting the interaction between fascin and microtubules does not significantly impact on fascin F-actin binding. We further show that S274 is a key residue in fascin regulating microtubule binding and that a phospho-mimicking mutation of this residue results in highly stable MT binding. Disruption of the fascin-MT complex leads to reduced focal adhesion disassembly and impaired cell migration through control of FAK/Src signalling. Our data support a model whereby fascin-actin bundling and fascin-MT binding act in synergy to control FA dynamics and cell motility (Fig 7). We propose that phosphorylation of S274 can potentially disrupt the interface between F-actin and the actin bundling site located between beta trefoils-2 and -3 in fascin, thus revealing the MT1 binding site located on the adjacent beta-trefoil 2 domain and promoting the switch from F-actin to MT binding (Fig 7). The available crystal structures of fascin (Jansen et al., 2011) show that the MT1 binding site we have identified is exposed within the molecule, further supporting our hypothesis that F-actin bundling provides a potential mask across this domain to prevent MT engagement with fascin. Our data also provides new

regions of fascin to explore for rational design for agents that target fascin-actin and fascin-MT binding and potentially target cancer cell metastasis.

Microtubules have previously been shown to promote adhesion disassembly, through delivery of disassembly or relaxation factor(s) and/or through activation of the Rho family GTPases (Ezratty et al., 2005; Palazzo et al., 2004; Waterman-Storer et al., 1999). Our data demonstrates that fascin can be found in a complex with FAK, and the complex formation is coincident with a transient re-localisation to peripheral adhesion sites. Moreover, fascin is required for normal MT dynamics and that loss of fascin leads to a more stable MT network. These observations strongly suggest that fascin can associate with distinct, specific binding partners within different subcellular sites depending on phosphorylation status at both N and C terminal sites. Our data would further support the concept that fascin that is phosphorylated at S274 preferentially locates at peripheral membrane sites. Our study additionally shows that expression of fascin mutants that bind to MT and suppress MT dynamics also result in reduced active FAK and Src levels at adhesion sites. Our finding that defective adhesion disassembly in cells expressing S274D or MT1 fascin can be rescued by expression of constitutively active Src would suggest that fascin acts upstream of the FAK-Src complex. Interestingly, stable MT networks have also been proposed to transmit mechanical stress signals to activate Src at focal adhesions, providing a further potential explanation of how fascin may regulate this pathway (Na et al., 2008). Notably we did not detect significant levels of fascin directly within focal adhesions by fluorescence confocal microscopy or TIRF microscopy in MDA MB 231 cells, HeLa cells or NIH 3T3 fibroblasts under basal conditions. In agreement with our findings, none of the previous studies have reported adhesion localisation of endogenous or overexpressed fascin in a wide range of normal and transformed cells (Anilkumar et al., 2003; Jansen et al., 2011; Ross et al., 2000; Schoumacher et al., 2014; Vignjevic et al., 2006; Yamakita et al., 1996; Yang et al., 2013). This wealth of data suggests that fascin is not a common component of focal adhesions; one exception being a recent study demonstrating fascin recruitment to adhesions in HCT116 cells perhaps due to specific differences in the motile or contractile behaviour of these cells (Elkhatib et al., 2014). However, we have shown that fascin can be transiently recruited to focal adhesions at low levels following nocodazole washout when cells are actively disassembling adhesions and microtubules are highly dynamic. This model is further supported by a very recent proteomics study showing fascin is one of a large family of proteins that are specifically enriched in complexes with active integrins (Byron et al., 2015). Thus it seems likely that fascin is transiently associated with populations of active adhesion molecules through a so-called ‘kiss-and-run’ mechanism and this is controlled through relative affinities for F-actin and microtubule cytoskeletons.

There are a number of mechanisms that may control local changes in fascin binding to different cytoskeletal networks during migration. We have recently shown that activation of the RhoA-ROCK-LIMK signalling pathway promotes fascin-actin bundling through a direct association between fascin and LIMK

within filopodia (Jayo et al., 2012). Control of microtubule stability by fascin has the potential to act as a feedback loop to regulate fascin function. Recent studies have shown that the RhoA exchange factor GEF-H1 is released from MT and activated following MT destabilization leading to enhanced RhoA activity that in turn promotes invasion within dense 3D collagen matrices (Chang et al., 2008; Heck et al., 2012). Local activation of RhoA following MT destabilization may therefore favour a switch from fascin-MT to fascin-actin association and thus promote actin assembly and membrane protrusion. Recent reports have shown that a dynamic MT network is required for membrane associated PKC activation and active PKC then promotes association of EB1 and KIF17 with growing MT plus tips (Espenel et al., 2013; Nakhost et al., 2002; Schober et al., 2012). As PKC is known to act on fascin to promote a non-actin bundling conformation through phosphorylation on S39, it is possible that an active pool of PKC proximal to MT +tips would also potentially favour local fascin disconnection from F-actin bundles.

Fascin has previously been shown to promote migration and invasion of cancer cells, the assumption being that this was mediated entirely through fascin-actin dependent control of filopodia and invadopodia structures (Hashimoto et al., 2007; Li et al., 2010; Schoumacher et al., 2010). Our current data suggests that fascin may also contribute to these processes through regulating MT dynamics and adhesion stability. Previous studies have shown that stable MT can be concentrated towards the leading edge of polarized cells or within matrix-degrading adhesions and this contributes to directed cell migration and chemotaxis (Diaz-Valencia et al., 2011; Montagnac et al., 2013; Schoumacher et al., 2010; Wu et al., 2008). Each cytoskeletal network plays a distinct role in cellular architecture, plasticity and responses to a changing extracellular environment but the way in which this is co-ordinated remains poorly understood. Given that fascin is now a widely recognized prognostic marker of metastatic disease, it will be important to investigate in future whether strategies targeted towards dual inhibition or modulation of fascin-actin and fascin-MT binding can slow or restrict invasive disease.

## Materials and Methods

### *Reagents and antibodies*

Antibodies were purchased from the following suppliers: mouse anti-β-tubulin, mouse anti-acetylated tubulin, mouse anti-PY and mouse anti-vinculin were all from Sigma-Aldrich (St Louis, MA, USA); rabbit anti-α/β Tubulin and mouse anti-Src were from Cell Signaling Technology (Danvers, MA, USA); mouse anti-fascin and anti-mouse/rabbit-HRP conjugated secondary antibodies were from Dako (Cambridge, UK); mouse anti-FAK was from Santa Cruz Biotechnology (Santa Cruz, CA, USA); anti-Y397FAK and all Alexa dye conjugated secondary antibodies and Phalloidin were from Invitrogen (Carlsbad, CA, USA). Nocodazole, Taxol and Cytochalasin D were obtained from Sigma Aldrich (St Louis, MA, USA).

***Cell culture and transfection***

MDA-MB-231 human breast carcinoma, 293T and HeLa cervical cancer cells were maintained at 37 ºC in Dulbecco's Modified Eagle's Medium (DMEM; Sigma Aldrich; St Louis, MA, USA)) with 4500 mg glucose/L supplemented with 10% fetal bovine serum (FBS; Sera Laboratories), 1% L-Glutamine and 1% penicillin/streptomycin (both from Gibco UK). NIH3T3 cells were maintained in DMEM with 10% newborn calf serum (NCS). Cells were transfected in Optimem serum free media (Gibco, UK) using Lipofectime transfection reagent according to manufacturers instructions (Invitrogen Life Technologies, UK).

***Fly stocks***

We used the following lines obtained from the Bloomington *Drosophila Melanogaster* Stock Center and the community: $sn^{28}$, upstream activation sequence (UAS)-GFP-Fascin (Zanet et al., 2009), UAS-mCherry-Fascin (Zanet et al., 2012b), UAS-GFP-Clip and UAS-Spastin-GFP (Stramer et al., 2010).

***Plasmids, cloning and virus production***

Human lentiviral short hairpin RNA (shRNA) targeting fascin was cloned into the pLentiLox 3.7 (LL3.7), kindly donated by Dr Adams (University of Bristol, UK). The sequence of the shRNA (gift from Dr Monypenny, KCL) used to knock down fascin was 5'-GCCTGAAGAAGAAGCAGAT-3' directed to the first exon of the human fascin gene, isoform 1 (FSCN1). Additionally, a scrambled sequence of the shRNA was cloned into the LL3.7 vector and used as a control. Scrambled and fascin targeting shRNA sequences were also cloned into a pLKO lentiviral vector (RNAi Consortium) between the *AgeI* and *EcoRI* sites. shRNA-resistant hfascin cDNA in which the shRNA target sequence was changed to 5'-GCCTGAAAAAAAAACAGAT-3' (underlined letter indicate changes) and its wild type and mutant forms were generated and tagged in the N terminal site with pEGFP (Clontech). The four single Fascin mutant forms (Ser39 and 274) were mutated to either a non-phosphorylatable alanine (A) or a phospho-mimic aspartic acid (D) and were generated as described in (Zanet et al., 2012a). Double mutant fascins were generated through mutation of the S274 in the S39 mutant background. For recombinant fascin purification, the cDNA encoding hfascin wild type and mutants were cloned between *NotI* and *XhoI* restriction sites in the p-ET30a(+) vector (Novagen, UK). Fascin MT1 and delMT1 mutants were generated on the pEGFP-fascin and p-ET30a-fascin backbones by site directed mutagenesis using the following oligos: 5'- CCC GCC GGC GCG CTC GCG GCG GGC GCG GCC ACC AAG GTG GGC-3' and 5'-CCC GCC TTG AGC GCG CCG GCG GGC CCC GCC GGC GCC AGG TAA C-3' for MT1 and 5'- CGT TAC CTG GCG CCG GAC GAG CTC TTT GCT C-3' and 5'- GAG CAA AGA GCT CGT CCG GCG CCA GGT AAC G-3' for delMT1. Vinculin-mRFP was as described previously {Worth, 2010 #220}. The human $\alpha$-tubulin cDNA was cloned in m-Cherry tagged lentiviral vector pLVX (gift from Dr James Monypenny, King's College London, UK) between *XhoI* and *BamHI-HF* sites. The following primers were used for PCR: 5'-CTC GAG GGA GGT GGA ATG CGT GAG TGC ATC TCC AT-3'; 5'-GGA TCC TTA GTA TTC CTC TCC TCT T-3'. The

cDNAs encoding the GST tagged FERM domain, kinase and C-terminal domain of Focal Adhesion Kinase were generated by Prof Margaret Frame (University of Edinburgh, UK). Lentivirus was produced and cells infected as described previously (Scales et al., 2013).

***Protein purification and pulldowns***

BL21 cells containing DNA of interest were grown overnight at 37°C. The culture was diluted (1:100) with fresh broth and cells grown at 37°C in a shaking incubator for 3-4 hrs. Protein production was induced with Isopropyl β-D-1-thiogalactopyranoside (IPTG, 0.2 mM) and incubated for a further 3-4 hrs. The bacterial culture was pelleted by centrifuging at 3900 rpm for 15 mins, 4°C. The pellet was then resuspended in 50 µl ice cold PBS per ml of original culture volume, containing protease inhibitors (Calbiochem, UK) and disrupted by sonication 10 x 10 seconds with pause of 10 seconds (on ice) at 10 A. The solution was centrifuged at 3900 rpm for 30 mins at 4°C and the supernatant collected. Ni-NTA agarose beads (Qiagen, UK) were packed on Chromatography disposable columns (Thermo Scientific) and washed with Lysis Buffer (50 mM Sodium Phosphate, 10 mM Imidazole, 300 mM Sodium Chloride (pH 8). Subsequently, beads were added to the supernatant to 5 µl beads/1 ml original culture and left to mix overnight at 4°C. The beads were spun down and washed with buffers containing increasing concentration of Imidazole. A high concentration of Imidazole was used to elute the proteins. The eluted protein was dialysed against Storage Buffer (PBS 1x, 10 mM Imidazole, 10% Glycerol (pH 8) for at least 2 hours at 4 ºC. Proteins were recovered and used for further experiments. Stocks of protein were kept at -80 ºC and SDS-PAGE was run to check protein purification. Silver or coomassie staining was used to detect binding in MT/actin co-sedimentation experiments.

***Western Blotting***

Samples for western blotting were prepared from cell lysates, pulldown and/or immunoprecipitation experiments. The protein samples were run on SDS PAGE gels and membranes probed with the primary antibody overnight at 4 ºC or for 3 hrs at room temperature. The membranes were then washed 3 times for 10 mins each with PBS-Tween (0.1% Tween in PBS) prior to incubation with horseradish peroxidase-conjugated secondary antibodies for 1 hr at room temperature. Membranes were then washed a further 3 times and proteins were detected by ECL chemiluminescence kit (Thermo Scientific, UK) on a BioRad imager. For reprobing, blots were stripped with Re-blot strong (10X) (Chemicon) diluted to 1X in distilled water for 10 mins at room temperature, and then blocked and incubated with antibodies as before.

***Immunoprecipitation***

Control or fascin knockdown MDA-MB-231 cells expressing GFP-WT or mutant fascin were lysed in 250 µl 50 mM Tris (pH7.2), 150 mM NaCl, 1 mM EDTA, 1% Triton X-100, PI cocktail, phosphatase inhibitors: 50 mM sodium fluoride and 1 µM calyculin on ice. Lysates were pre-cleared with 50 µl washed A/G agarose affinity

matrix suspension rotating at 4 ºC for 30 mins, and 50 µl of lysate was kept. A/G agarose affinity matrix suspension was washed 3 times with cold PBS prior to use. Antibody or control IgG was pre-incubated with beads for 3 hours tumbling at 4 ºC. Then, excess antibody was removed by washing 3 times with PBS, and pre-cleared lysate was added to each antibody A/G agarose affinity matrix suspension mix overnight tumbling at 4 ºC. A/G agarose affinity matrix suspension was washed three times for 10 mins in IP buffer. Lysates were boiled at 95 ºC and centrifuged to clear cell debris before use. 40 µl of each sample was loaded in each well of 8 or 10% SDS-PAGE gels and subjected to SDS-PAGE, followed by western blotting. Each IP was performed at least 3 times and quantified using densitometry analysis.

***MT and Actin sedimentation analysis***

For MT analysis, Bovine brain tubulin (Cytoskeleton) was diluted in General Tubulin Buffer (GTB; 50 mM PIPES (pH 6.8), 1 mM EGTA, 1 mM Magnesium Chloride) at a final concentration of 10 µg/µl. 5 µg of purified tubulin was polymerised for 15 mins at 37 ºC in Tubulin Polymerisation Buffer (GTB, 10% Glycerol, 5 mM Magnesium Chloride, 1 mM GTP). Increasing concentrations of Taxol (Sigma) were added every 10 mins. MT structure was confirmed by electron microscopy. The mixture was then layered onto 60 µl of Tubulin Pelleting Buffer (GTB, 50% Glycerol, 1mM GTP, 80 uM Taxol) and centrifuged at 13,000 rpm for 20 mins at 25 ºC. The buffer was prepared in 50% Glycerol, which allows polymerised tubulin (MT) sedimentation. The MT pellet was resuspended in 60 µl of GTB plus 1 mM GTP, 80 uM Taxol. Polymerised tubulin corresponding to approximately 5 µg (1 µmol) was incubated with $His_6$ tagged WT or mutant fascin protein (1:1 ratio) in GTB for 30 mins at 25 ºC. Each reaction mixture was then layered onto 20 µl of GTB and reactions were centrifuged at 13,000 rpm for 30 mins at 25 ºC. As a control, MT, WT and mutant fascin proteins were subjected to centrifugation alone in every co-sedimentation experiment. 5x Loading Buffer was added to supernatants (unbound fraction), while each pellet was resuspended in 40 µl of GTB (15% Glycerol was added to GTB) and 2x Loading Buffer was added. The supernatant (s) and pellet (p) fractions were recovered by SDS-PAGE and stained with Silver staining. Protein bands were quantified by densitometry. F-actin co-sedimentation experiments with fascin were carried out as previously described (Zanet et al., 2012b). Protein bands were quantified by densitometry.

***Confocal microscopy and image analysis:***

For Nocodazole washout assays, cells were treated with Nocodazole or DMSO (control) (Sigma Aldrich) at 10 µM diluted in 10% FBS DMEM media for 15 mins to completely disassemble MT. After treatment, cells were either fixed and stained immediately or the Nocodazole was washed out and replaced with fresh 10% FBS DMEM media for 30 or 60 mins to allow MT re-growth followed by fixation with PFA. The cells were stained with antibodies for total tubulin or phospho-tyrosine (PY) or vinculin and imaged with confocal microscopy. For live cell imaging of focal adhesion dynamics, specified cells expressing vinculin-mRFP were plated into glass-bottomed imaging chambers (Ibidi) in phenol red free media containing Nocodazole and

subjected to time-lapse confocal microscopy before and after Nocodazole washout. Resulting NIS Elements ND2 files were exported and used for analysis in ImageJ for focal adhesion area/cell area as for fixed samples. Images of cells stained for total tubulin were scored for percentage of cells with normal MT network (MT score). Images were thresholded in ImageJ and binarised to define MT network followed by overlay of cell boundary using phalloidin co-staining to define cell edges. Cells exhibiting polymerised MT bundles, distributed throughout the cell body to the entire periphery of the cell with a visible MT organising centre (MTOC) were scored 100% re-growth. Spreading cells exhibiting an MT network that was incompletely re-grown were scored according to the MT coverage as a function of cell area (between 95 and 5%); cells exhibiting a largely depolymerised or diffuse MT network or with only a visible MTOC present scored as 5% or below. MT re-growth was calculated as a function of cell area, thus controlling for smaller spread area detected in fascin depleted cells. Quantification of cell size and focal adhesion (FA) size and number was performed by application of a threshold to all images using ImageJ to isolate and identify FA between 1 and 5 μm in size. FA size data was normalised to total cell area and presented as % of cell occupied by FA. In all the analysis, at least 40 cells were evaluated in three different experiments. N numbers for each are defined in associated figure legends. Quantification of filopodia number was performed on confocal images of live cells co-expressing GFP-fascin (WT and mutants) and lifeact-mRFP. Filopodia were defined as membrane projections protruding more than 2 microns from the plasma membrane and containing F-actin and fascin. Images were acquired from multiple live cells and filopodia number and length per cell were quantified from these images using ImageJ and averaged across multiple cells and experiments.

***FRET/FLIM:***

Fluorescence resonance energy transfer (FRET) was measured using Fluorescence lifetime imaging microscopy (FLIM) as previously described [13]. Histogram data are plotted as mean FRET efficiency per cell, pooled from specified numbers of cells and experiments as detailed in figure legends. ANOVA was used to test statistical significance between different populations of data. Lifetime images of example cells are presented using a pseudocolor scale, whereby blue depicts normal GFP lifetime (no FRET) and red depicts lower GFP lifetime (areas of FRET where proteins are within <10nm proximity).

***Live imaging of Drosophila embryos***

UAS transgenic constructs encoding fluorescent proteins were expressed specifically in macrophages using the *singed*-Gal4 driver line (Zanet et al., 2012a). Live embryos were mounted as previously described (Wood et al., 2006). Briefly, Stage 15 embryos were dechorionated in bleach and mounted under coverslips on hydrophobic Lumox dishes (Sarstedt, Germany) in Voltalef oil 10S. Embryos were then imaged with a spinning disk microscope (UltraVIEW VoX PerkinElmer) with a 63× N.A. 1.4 objective acquiring one image/30s. Measurements of the length of fascin bundles were performed using Volocity software. MT

arms were defined as polarised bundles of MT that anticipate direction of migration as previously described in (Stramer et al., 2010).

***Microtubule imaging and tracking***

Time-lapse movies of HeLa cells expressing tubulin-RFP were acquired on an Olympus IX71 epifluorescent microscope equipped with EMCCD camera (Ixon, Andor, Belfast) using a 60x 1.42 N.A. oil objective. To track single microtubules at cell periphery, acquired movies were subjected to a bandpass filter (20:2 pixels) in ImageJ (NIH), background subtracted using a rolling ball radius of 15 pixels, and a 3D Gaussian blur filter applied. Resulting movies were overlaid with the originals to avoid image processing-derived artefacts and single microtubule length was measured over time from a defined starting point proximal to cell periphery. Frequency of catastrophe, growth rate and time spent in growth phase were quantified.

***Statistical analysis***

All statistical tests were performed using Students T-test (Excel) or ANOVA (Prism) as relevant for specified data sets. Data are expressed as means ± SEM. Experimental and cell (where relevant) N numbers are detailed in associated figure legends. Significance was taken as $p<0.001$, 0.005 and 0.05 and significance values were assigned in specific figures/experiments as detailed in individual figure legends.

**References**


Anilkumar, N., M. Parsons, R. Monk, T. Ng, and J.C. Adams. 2003. Interaction of fascin and protein kinase Calpha: a novel intersection in cell adhesion and motility. *Embo J*. 22:5390-5402.

Bi, J., X. Chen, Y. Zhang, B. Li, J. Sun, H. Shen, and C. Kong. 2012. Fascin is a predictor for invasiveness and recurrence of urothelial carcinoma of bladder. *Urol Oncol*. 30:688-694.

Byron, A., J.A. Askari, J.D. Humphries, G. Jacquemet, E.J. Koper, S. Warwood, C.K. Choi, M.J. Stroud, C.S. Chen, D. Knight, and M.J. Humphries. 2015. A proteomic approach reveals integrin activation state-dependent control of microtubule cortical targeting. *Nat Commun*. 6:6135.

Cao, B., and C. Mao. 2009. Identification of microtubule-binding domains on microtubule-associated proteins by major coat phage display technique. *Biomacromolecules*. 10:555-564.

Chang, Y.C., P. Nalbant, J. Birkenfeld, Z.F. Chang, and G.M. Bokoch. 2008. GEF-H1 couples nocodazole-induced microtubule disassembly to cell contractility via RhoA. *Mol Biol Cell*. 19:2147-2153.

Ciobanasu, C., B. Faivre, and C. Le Clainche. 2013. Integrating actin dynamics, mechanotransduction and integrin activation: the multiple functions of actin binding proteins in focal adhesions. *Eur J Cell Biol*. 92:339-348.

Diaz-Valencia, J.D., M.M. Morelli, M. Bailey, D. Zhang, D.J. Sharp, and J.L. Ross. 2011. Drosophila katanin-60 depolymerizes and severs at microtubule defects. *Biophys J*. 100:2440-2449.

Elkhatib, N., M.B. Neu, C. Zensen, K.M. Schmoller, D. Louvard, A.R. Bausch, T. Betz, and D.M. Vignjevic. 2014. Fascin plays a role in stress fiber organization and focal adhesion disassembly. *Current biology : CB*. 24:1492-1499.

Espenel, C., B.R. Acharya, and G. Kreitzer. 2013. A biosensor of local kinesin activity reveals roles of PKC and EB1 in KIF17 activation. *J Cell Biol*. 203:445-455.

Etienne-Manneville, S. 2013. Microtubules in cell migration. *Annu Rev Cell Dev Biol*. 29:471-499.

Ezratty, E.J., C. Bertaux, E.E. Marcantonio, and G.G. Gundersen. 2009. Clathrin mediates integrin endocytosis for focal adhesion disassembly in migrating cells. *J Cell Biol*. 187:733-747.

Ezratty, E.J., M.A. Partridge, and G.G. Gundersen. 2005. Microtubule-induced focal adhesion disassembly is mediated by dynamin and focal adhesion kinase. *Nat Cell Biol*. 7:581-590.

Gao, W., C. Zhang, Y. Feng, G. Chen, S. Wen, H. Huangfu, and B. Wang. 2012. Fascin-1, ezrin and paxillin contribute to the malignant progression and are predictors of clinical prognosis in laryngeal squamous cell carcinoma. *PLoS One*. 7:e50710.

Hamadi, A., M. Bouali, M. Dontenwill, H. Stoeckel, K. Takeda, and P. Ronde. 2005. Regulation of focal adhesion dynamics and disassembly by phosphorylation of FAK at tyrosine 397. *J Cell Sci*. 118:4415-4425.

Hashimoto, Y., M. Parsons, and J.C. Adams. 2007. Dual actin-bundling and protein kinase C-binding activities of fascin regulate carcinoma cell migration downstream of Rac and contribute to metastasis. *Mol Biol Cell*. 18:4591-4602.

Hashimoto, Y., M. Skacel, I.C. Lavery, A.L. Mukherjee, G. Casey, and J.C. Adams. 2006. Prognostic significance of fascin expression in advanced colorectal cancer: an immunohistochemical study of colorectal adenomas and adenocarcinomas. *BMC Cancer*. 6:241.

Heck, J.N., S.M. Ponik, M.G. Garcia-Mendoza, C.A. Pehlke, D.R. Inman, K.W. Eliceiri, and P.J. Keely. 2012. Microtubules regulate GEF-H1 in response to extracellular matrix stiffness. *Mol Biol Cell*. 23:2583-2592.

Jansen, S., A. Collins, C. Yang, G. Rebowski, T. Svitkina, and R. Dominguez. 2011. Mechanism of actin filament bundling by fascin. *J Biol Chem*. 286:30087-30096.

Jayo, A., and M. Parsons. 2010. Fascin: a key regulator of cytoskeletal dynamics. *Int J Biochem Cell Biol*. 42:1614-1617.

Jayo, A., M. Parsons, and J.C. Adams. 2012. A novel Rho-dependent pathway that drives interaction of fascin-1 with p-Lin-11/Isl-1/Mec-3 kinase (LIMK) 1/2 to promote fascin-1/actin binding and filopodia stability. *BMC Biol*. 10:72.

Klumpp, L.M., K.M. Brendza, J.M. Rosenberg, A. Hoenger, and S.P. Gilbert. 2003. Motor domain mutation traps kinesin as a microtubule rigor complex. *Biochemistry*. 42:2595-2606.

Li, A., J.C. Dawson, M. Forero-Vargas, H.J. Spence, X. Yu, I. Konig, K. Anderson, and L.M. Machesky. 2010. The actin-bundling protein fascin stabilizes actin in invadopodia and potentiates protrusive invasion. *Curr Biol*. 20:339-345.
Li, X., H. Zheng, T. Hara, H. Takahashi, S. Masuda, Z. Wang, X. Yang, Y. Guan, and Y. Takano. 2008. Aberrant expression of cortactin and fascin are effective markers for pathogenesis, invasion, metastasis and prognosis of gastric carcinomas. *Int J Oncol*. 33:69-79.
Makrantoni, V., S.J. Corbishley, N. Rachidi, N.A. Morrice, D.A. Robinson, and M.J. Stark. 2014. Phosphorylation of Sli15 by Ipl1 is important for proper CPC localization and chromosome stability in Saccharomyces cerevisiae. *PLoS One*. 9:e89399.
Montagnac, G., V. Meas-Yedid, M. Irondelle, A. Castro-Castro, M. Franco, T. Shida, M.V. Nachury, A. Benmerah, J.C. Olivo-Marin, and P. Chavrier. 2013. alphaTAT1 catalyses microtubule acetylation at clathrin-coated pits. *Nature*. 502:567-570.
Na, S., O. Collin, F. Chowdhury, B. Tay, M. Ouyang, Y. Wang, and N. Wang. 2008. Rapid signal transduction in living cells is a unique feature of mechanotransduction. *Proc Natl Acad Sci U S A*. 105:6626-6631.
Nakhost, A., N. Kabir, P. Forscher, and W.S. Sossin. 2002. Protein kinase C isoforms are translocated to microtubules in neurons. *J Biol Chem*. 277:40633-40639.
Ono, S., Y. Yamakita, S. Yamashiro, P.T. Matsudaira, J.R. Gnarra, T. Obinata, and F. Matsumura. 1997a. Identification of an actin binding region and a protein kinase C phosphorylation site on human fascin. *J Biol Chem*. 272:2527-2533.
Ono, S., Y. Yamakita, S. Yamashiro, P.T. Matsudaira, J.R. Gnarra, T. Obinata, and F. Matsumura. 1997b. Identification of an actin binding region and a protein kinase C phosphorylation site on human fascin. *J Biol Chem*. 272:2527-2533.
Palazzo, A.F., C.H. Eng, D.D. Schlaepfer, E.E. Marcantonio, and G.G. Gundersen. 2004. Localized stabilization of microtubules by integrin- and FAK-facilitated Rho signaling. *Science*. 303:836-839.
Ross, R., H. Jonuleit, M. Bros, X.L. Ross, S. Yamashiro, F. Matsumura, A.H. Enk, J. Knop, and A.B. Reske-Kunz. 2000. Expression of the actin-bundling protein fascin in cultured human dendritic cells correlates with dendritic morphology and cell differentiation. *J Invest Dermatol*. 115:658-663.
Scales, T.M., A. Jayo, B. Obara, M.R. Holt, N.A. Hotchin, F. Berditchevski, and M. Parsons. 2013. alpha3beta1 integrins regulate CD151 complex assembly and membrane dynamics in carcinoma cells within 3D environments. *Oncogene*. 32:3965-3979.
Schaar, B.T., K. Kinoshita, and S.K. McConnell. 2004. Doublecortin microtubule affinity is regulated by a balance of kinase and phosphatase activity at the leading edge of migrating neurons. *Neuron*. 41:203-213.
Schober, J.M., G. Kwon, D. Jayne, and J.M. Cain. 2012. The microtubule-associated protein EB1 maintains cell polarity through activation of protein kinase C. *Biochem Biophys Res Commun*. 417:67-72.
Schoumacher, M., F. El-Marjou, M. Lae, N. Kambou, D. Louvard, S. Robine, and D.M. Vignjevic. 2014. Conditional expression of fascin increases tumor progression in a mouse model of intestinal cancer. *Eur J Cell Biol*.
Schoumacher, M., R.D. Goldman, D. Louvard, and D.M. Vignjevic. 2010. Actin, microtubules, and vimentin intermediate filaments cooperate for elongation of invadopodia. *J Cell Biol*. 189:541-556.
Shonukan, O., I. Bagayogo, P. McCrea, M. Chao, and B. Hempstead. 2003. Neurotrophin-induced melanoma cell migration is mediated through the actin-bundling protein fascin. *Oncogene*. 22:3616-3623.
Stramer, B., S. Moreira, T. Millard, I. Evans, C.Y. Huang, O. Sabet, M. Milner, G. Dunn, P. Martin, and W. Wood. 2010. Clasp-mediated microtubule bundling regulates persistent motility and contact repulsion in Drosophila macrophages in vivo. *J Cell Biol*. 189:681-689.
Vignjevic, D., S. Kojima, Y. Aratyn, O. Danciu, T. Svitkina, and G.G. Borisy. 2006. Role of fascin in filopodial protrusion. *J Cell Biol*. 174:863-875.
Wang, Y., H. Cao, J. Chen, and M.A. McNiven. 2011. A direct interaction between the large GTPase dynamin-2 and FAK regulates focal adhesion dynamics in response to active Src. *Mol Biol Cell*. 22:1529-1538.

Waterman-Storer, C.M., R.A. Worthylake, B.P. Liu, K. Burridge, and E.D. Salmon. 1999. Microtubule growth activates Rac1 to promote lamellipodial protrusion in fibroblasts. *Nat Cell Biol*. 1:45-50.
Webster, D.R., and G.G. Borisy. 1989. Microtubules are acetylated in domains that turn over slowly. *J Cell Sci*. 92 ( Pt 1):57-65.
Wood, W., C. Faria, and A. Jacinto. 2006. Distinct mechanisms regulate haemocyte chemotaxis during development and wound healing in Drosophila melanogaster. *J Cell Biol*. 173:405-416.
Wu, X., A. Kodama, and E. Fuchs. 2008. ACF7 regulates cytoskeletal-focal adhesion dynamics and migration and has ATPase activity. *Cell*. 135:137-148.
Yamakita, Y., S. Ono, F. Matsumura, and S. Yamashiro. 1996. Phosphorylation of human fascin inhibits its actin binding and bundling activities. *J Biol Chem*. 271:12632-12638.
Yang, S., F.K. Huang, J. Huang, S. Chen, J. Jakoncic, A. Leo-Macias, R. Diaz-Avalos, L. Chen, J.J. Zhang, and X.Y. Huang. 2013. Molecular mechanism of fascin function in filopodial formation. *J Biol Chem*. 288:274-284.
Zanet, J., A. Jayo, S. Plaza, T. Millard, M. Parsons, and B. Stramer. 2012a. Fascin promotes filopodia formation independent of its role in actin bundling. *J Cell Biol*. 197:477-486.
Zanet, J., A. Jayo, S. Plaza, T. Millard, M. Parsons, and B. Stramer. 2012b. Fascin promotes filopodia formation independent of its role in actin bundling. *J Cell Biol*. 197:477-486.
Zanet, J., B. Stramer, T. Millard, P. Martin, F. Payre, and S. Plaza. 2009. Fascin is required for blood cell migration during Drosophila embryogenesis. *Development*. 136:2557-2565.
Zhang, J., M. Fonovic, K. Suyama, M. Bogyo, and M.P. Scott. 2009. Rab35 controls actin bundling by recruiting fascin as an effector protein. *Science*. 325:1250-1254.
Zhu, B., L. Zhang, J. Creighton, M. Alexeyev, S.J. Strada, and T. Stevens. 2010. Protein kinase A phosphorylation of tau-serine 214 reorganizes microtubules and disrupts the endothelial cell barrier. *Am J Physiol Lung Cell Mol Physiol*. 299:L493-501.

**Acknowledgments**

The authors are grateful to Dr Mark Holt for help with image analysis, Dr James Monypenny for help with lentiviral cloning and the Nikon Imaging Centre@King's for microscopy assistance. Funding was provided by The Royal Society, Breast Cancer Campaign (2009NovPhD31) and Medical Research Council (MR/J000647/1). The authors have no competing financial interests.

## Figures

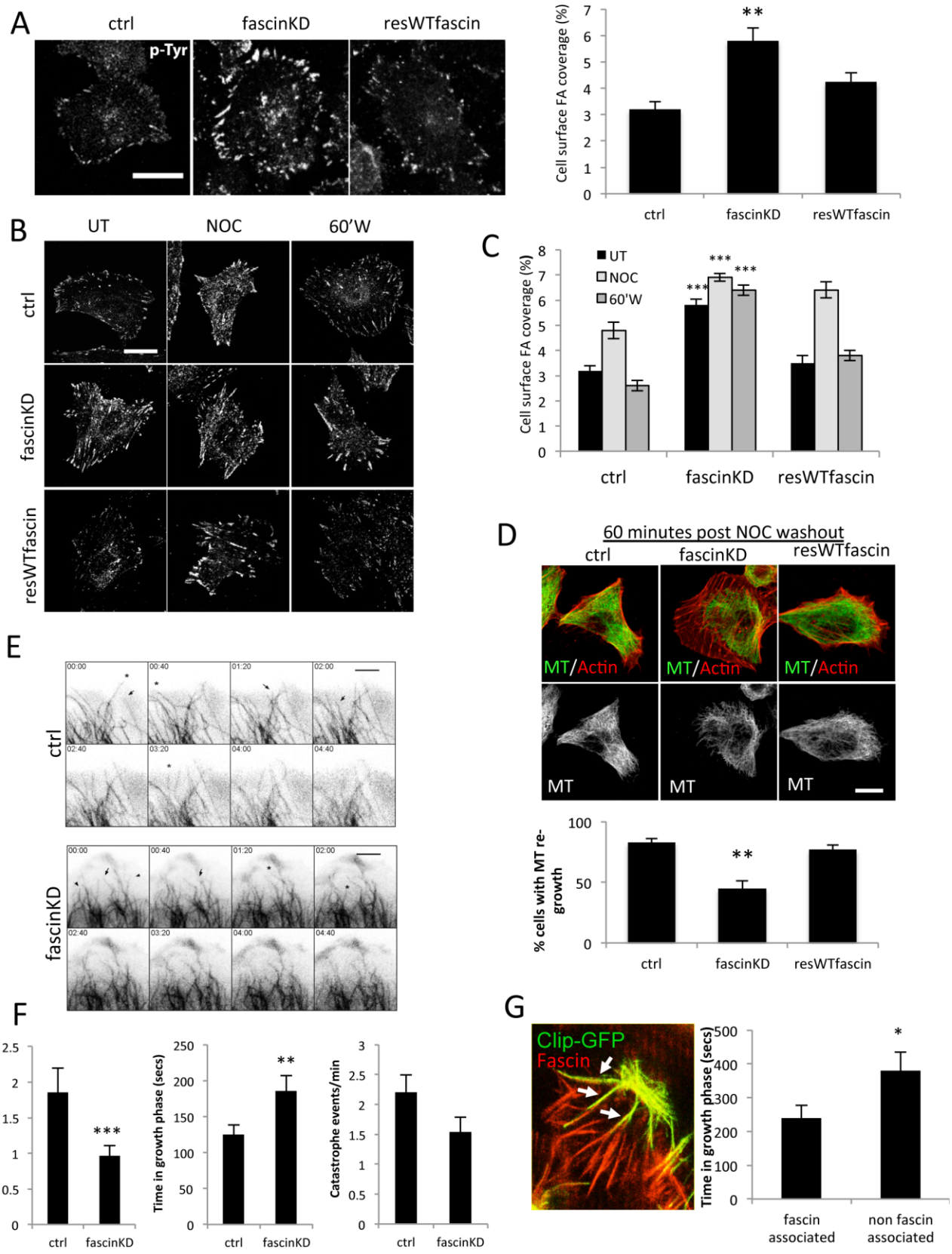

**Figure 1: Fascin regulates focal adhesion size and microtubule dynamics**

**(A)** Representative images of phosphotyrosine (p-Tyr) stained MDA MB 231 cells expressing control shRNA, fascinKD shRNA or fascinKD shRNA and WTfascin-GFP. Scale bar is 20 µm. Bar graph of quantification of % adhesion coverage area per cell calculated from 50 cells per condition over 3 independent experiments. **(B)** Representative images of MDA MB 231 cells as in (A) either untreated (UT), treated with Nocodazole for 20 minutes (NOC) or 60 minutes post-nocodazole washout (60'W). Scale bar is 20 µm. **(C)** Bar graph represents quantification of % cell surface covered by FA from images similar to those in (B) and represents adhesion area per cell calculated from 40 cells per condition over 3 independent experiments. **(D)** Example images of control or fascinKD cells stained for F-actin (red) or tubulin (green) following 60 minutes Nocodazole washout. Scale bars are 20 µm; graph below shows mean values of MT re-growth +/-SEM from n=30 cells per experiment. Images are representative of findings across 3 independent experiments. ***=$p<0.001$ compared to controls for equivalent conditions**. (E)** Example images taken from time-lapse confocal microscopy movies of control or fascinKD HeLa cells expressing tubulin-mCherry. Full movies are shown in Supplementary Movie1. Arrows and arrow-heads denote growing or stable MT respectively. Asterisks denote catastrophe events. **(F)** Bar graphs show quantification of microtubule growth rate, time spent in growth phase and microtubule catastrophe events per minute calculated from 15 MT per cell in 6 cells per experiment over 4 independent experiments. Bars show mean +/-SEM; **=$p<0.01$; ***=$p<0.001$**. (G)** Representative image of live Drosophila haemocytes within living embryos co-expressing mCherry-fascin and Clip-GFP. Arrows indicate regions of colocalisation between fascin and clip. Graph shows quantification from movies of live Drosophila haemocytes within living embryos co-expressing mCherry-fascin and Clip-GFP. Growth of fascin-associated and non-associated MT shown. Values are pooled from 95 MT analysed from 8 cells across 6 independent movies. Example time-lapse is shown in supplementary movie 2. Bars show mean +/-SEM; * = $p<0.05$.

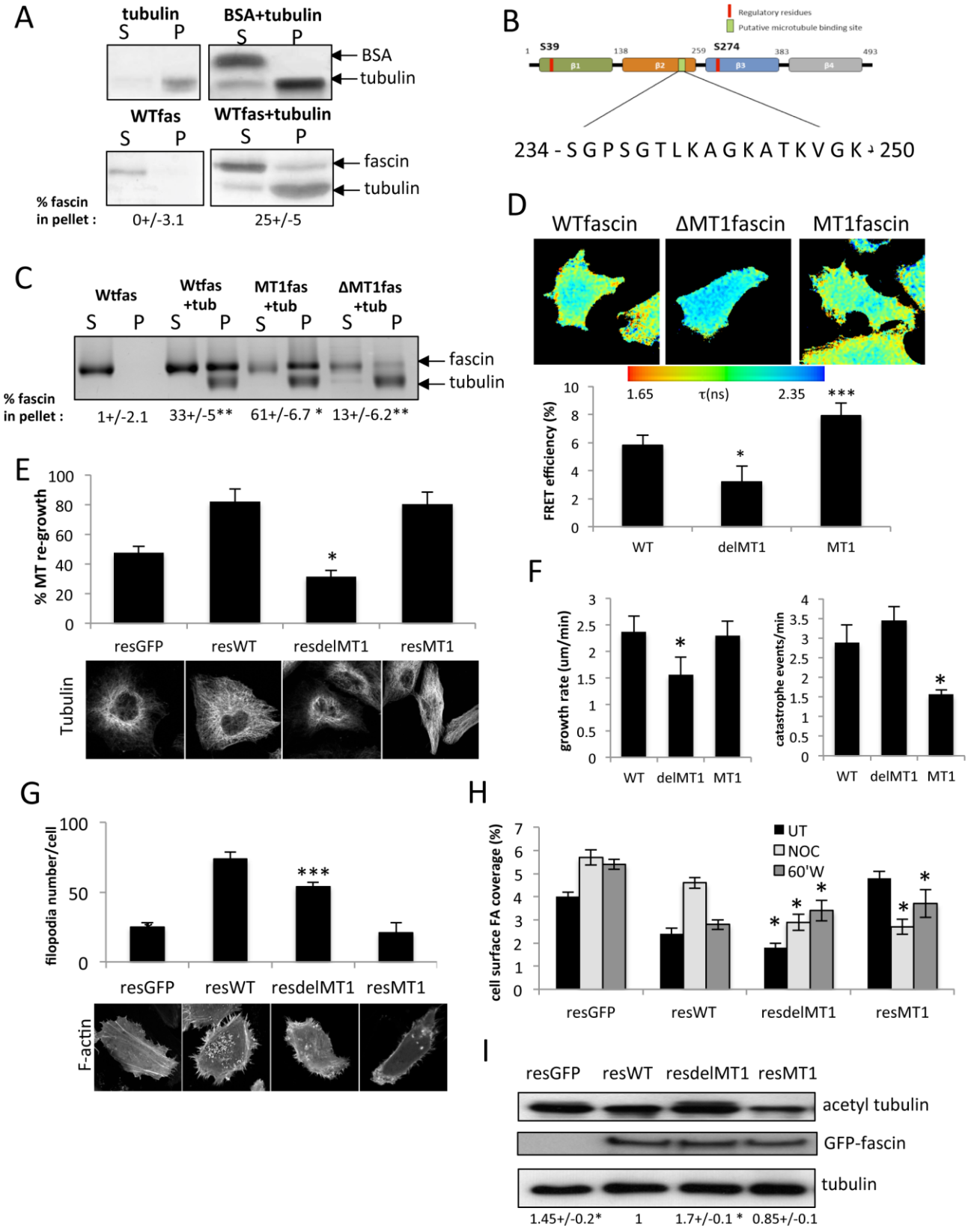


**Figure 2: Fascin binds to microtubules**

(**A)** Example images of silver stained gels showing levels of purified fascin or tubulin in the supernatant (S) or pellet (P) fractions following co-sedimentation. BSA was used as a protein control (top panel). Values beneath show % of fascin in pellet from 3 independent experiments +/-sem. **(B)** Schematic showing

identified putative MT1 binding domain in fascin. **(C)** Co-sedimentation analysis of purified WT vs mutant fascins with tubulin. MT1 denotes mutated fascin, ΔMT1 is deleted MT1 domain. Values beneath show % of fascin in pellet from 4 independent experiments +/-sem. **(D)** Example fluorescence lifetime maps of fascinKD cells expressing WT, ΔMT1 or MT1fascin-GFP and tubulin-mCherry. Pseudocolour lifetime scale is shown where warmer colours denote low lifetimes and therefore high FRET. Graph beneath shows quantification of FRET efficiency for each condition from 18 cells per condition over 3 independent experiments. Mean values +/-SEM are shown, *=p<0.01, ***=p<0.001 compared to WT. **(E)** Quantification of MT re-growth in HeLa fascinKD cells re-expressing GFP only or WT, ΔMT1 or MT1fascin-GFP following NOC washout for 60 minutes. Fixed cells stained with tubulin antibodies were scored as in Fig1. Example images are shown below the graph. **(F)** Analysis of MT growth rate (left graph) and catastrophe events/min (right graph) in fascinKD HeLa cells re-expressing WT, ΔMT1 or MT1fascin-GFP. Values are calculated from 25 MT per cell in 5 cells per experiment and 3 independent experiments. Example movies are shown in Supplementary Movie 3. **(G)** Quantification of filopodia number/cell in MDA MB 231 fascin knockdown cells re-expressing GFP alone, WTfascin-GFP or MT1/ΔMT1 mutants. Example images are shown below the graph. **(H)** Quantification of % FA surface area coverage of FascinKD cells expressing WT or MT1 mutant GFP-fascin during NOC washout. N=>35 cells quantified across 3 independent experiments. Mean values +/-SEM are shown, ***=p<0.001 compared to control equivalents. **(I)** Western blots of acetylated tubulin in HeLa fascin knockdown cells expressing GFP or specified fascin mutants. Blots were re-probed for GFP and tubulin. Numbers below blots are means +/-SEM from 3 experiments. *=p>0.005 vs WTfascin.

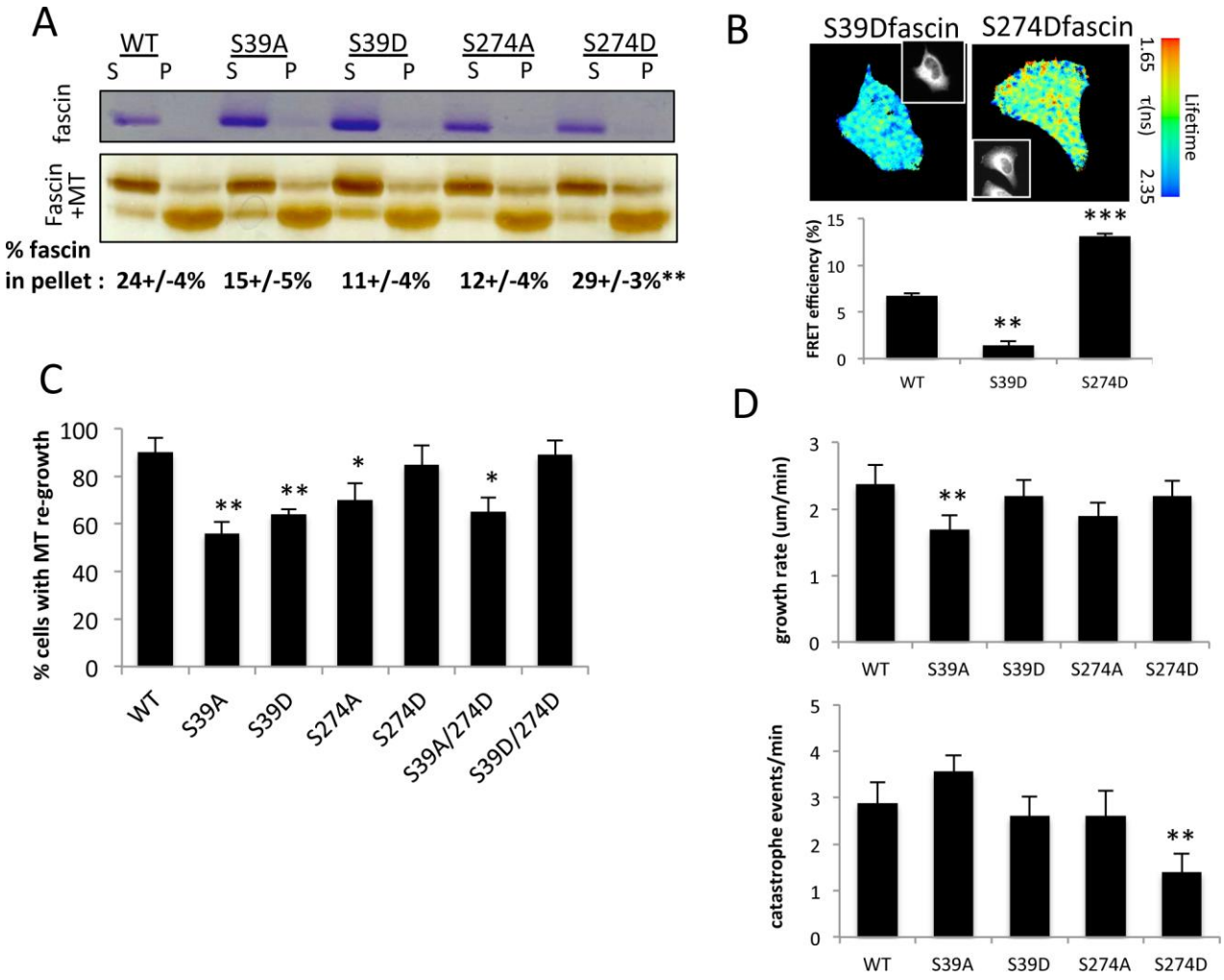


**Figure 3: Phosphorylation of fascin regulates MT and adhesion dynamics**

**(A)** Example images of coomassie and silver stained gels from co-sedimentation analysis of purified WT vs mutant fascin alone (top gel) or with tubulin (bottom gel) in supernatant (S) or pellet (P) fractions. Values beneath show % of fascin in pellet from 3 independent experiments +/-sem. **(B)** Example fluorescence lifetime maps of fascinKD cells expressing S39D or S274D fascin-GFP and tubulin-mCherry (shown in inset panels). Pseudocolour lifetime scale is shown next to each image. Graph shows quantification of FRET efficiency for WT, S39D and S274Dfascin-expressing cells from 15 cells per condition over 2 independent experiments. Mean values +/-SEM are shown, *=p<0.001 compared to WTfascin. **(C)** Quantification of microtubule re-growth from images of fixed MDA MB 231 FascinKD cells expressing WT or mutant GFP-fascin 60minutes post-NOC washout. N=30 cells were quantified across 3 independent experiments. **(D)** Analysis of MT growth rate (left graph) and catastrophe events/min (right graph) in fascinKD HeLa cells re-expressing WT or mutant GFP-fascin variants as specified. Values are calculated from 25 MT per cell in 5 cells per experiment over 3 independent experiments. Example movies are shown in Supplementary Movie 4.

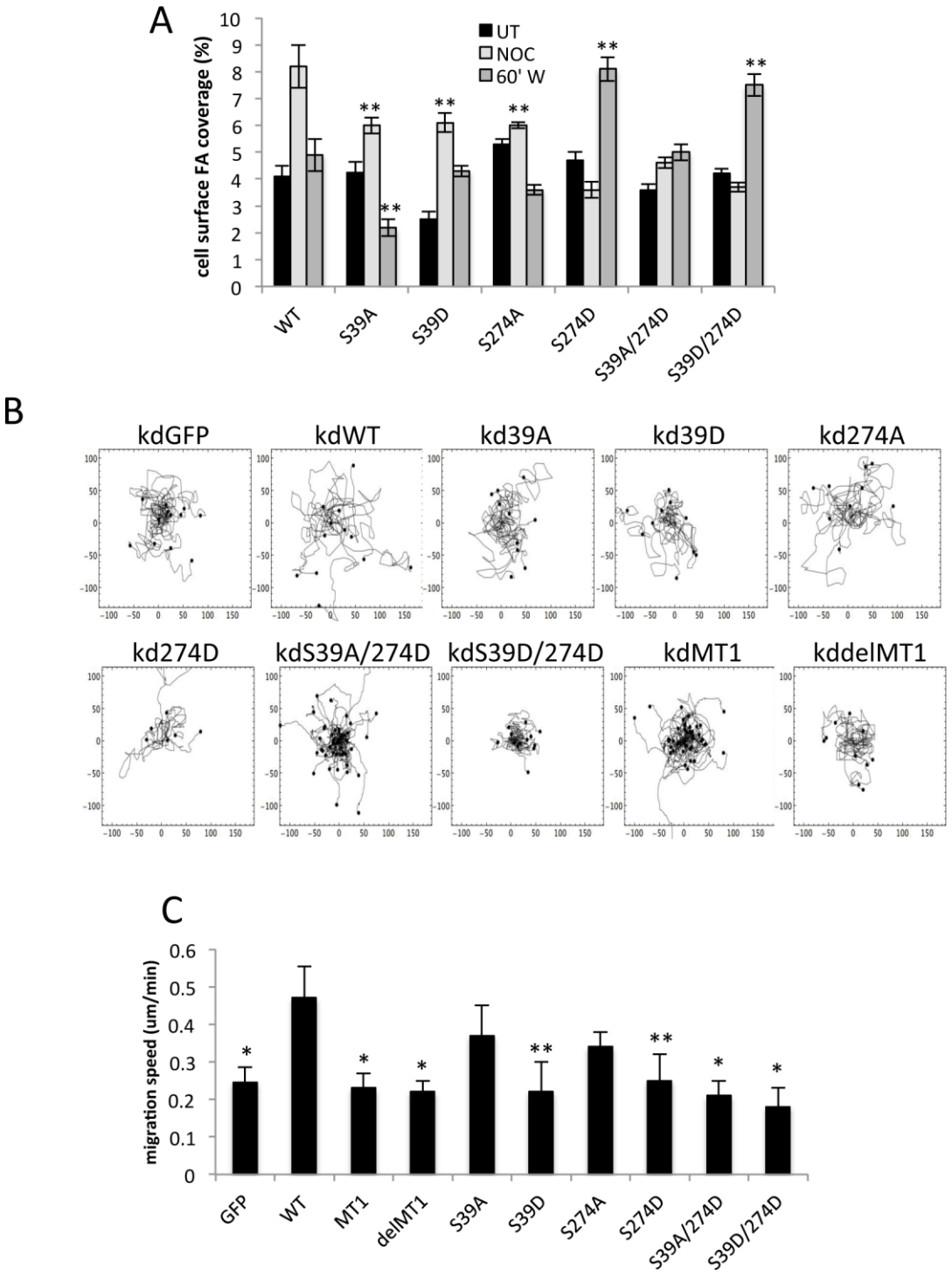


**Figure 4: Fascin-MT binding regulates cell adhesion dynamics and migration**

**(A)** Quantification of FA surface area coverage of MDA MB 231 FascinKD cells expressing WT or mutant GFP-fascin during NOC washout. N=45 cells were quantified across 3 independent experiments. **(B)** Example migration tracks of MDA MB 231 FascinKD cells expressing WT or mutant GFP-fascin taken from time-lapse movies. **(C)** Quantification of migration speed as determined from tracks as shown in (C). n=60 cells per condition. Mean values +/-SEM are shown; **=p<0.01; *=p<0.05 compared to scrGFP control equivalents.

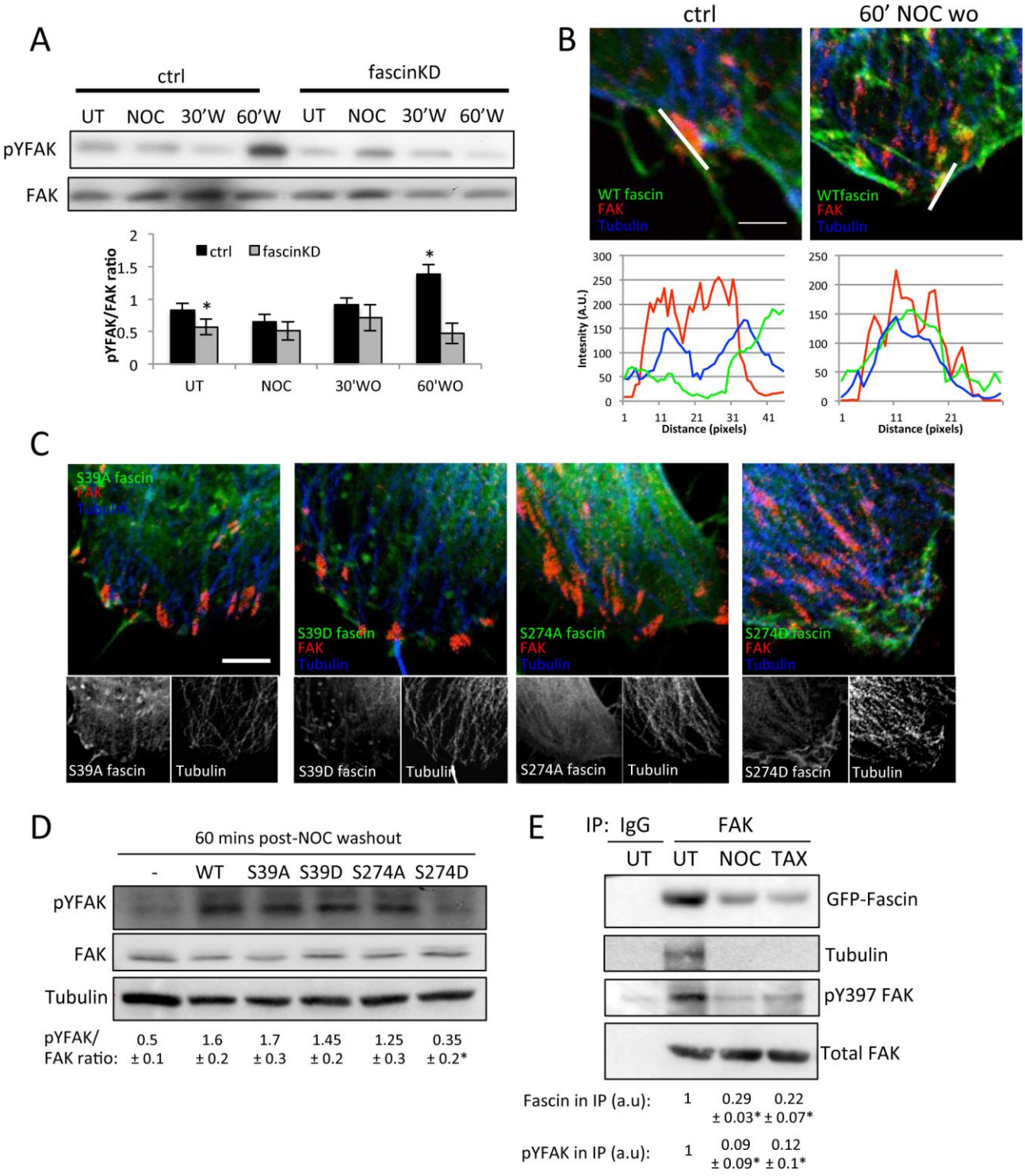


**Figure 5: Fascin regulates activation of FAK**

**(A)** Western blot of lysates from control and fascinKD MDA MB 231 cells either untreated (UT), 20 minutes following NOC treatment (NOC) or 30 or 60 minutes post NOC washout probed for pYFAK or total FAK. Graph beneath blots shows densitometry quantification of pY397-FAK/total FAK levels from 3 independent experiments. Mean values +/-SEM are shown, *=p<0.01 compared to control. **(B)** Representative confocal images of regions of control MDA MB 231 cells untreated (UT) or following NOC washout (60'W) fixed and stained for endogenous fascin (green), FAK (red) and tubulin (blue). Merged images are shown. Scale bar is

2 µm. **(C)** Example images of FAK staining (red) at focal adhesions at the periphery of fascinKD MDA MB 231 cells expressing specified fascin-GFP constructs (green) co-stained for tubulin (blue). Merged images are shown in top panels and fascin and tubulin channels shown as black and white images below. Scale bar is 15 µm. **(D)** Western blot of lysates from fascinKD or specified GFP-fascin rescued MDA MB 231 cells 60 minutes post Nocodazole washout, probed for pYFAK, FAK or tubulin. Numbers beneath blots are densitometry quantification of pY397-FAK/total FAK levels from 3 independent experiments. Mean values +/-SEM are shown, *=$p<0.01$ compared to control. **(E)** Western blots of lysates from control cells treated with Nocodazole (NOC) or Taxol and immunoprecipitated with control (IgG) or anti-FAK antibodies. Blots were probed for specified proteins. Relative fascin and p Y397FAK levels in each IP lane were quantified over 4 independent experiments. Values are denoted below each respective lane and represent relative intensity of each band as a mean of the 4 experiments +/-SEM. *=$p<0.001$ compared to untreated controls.

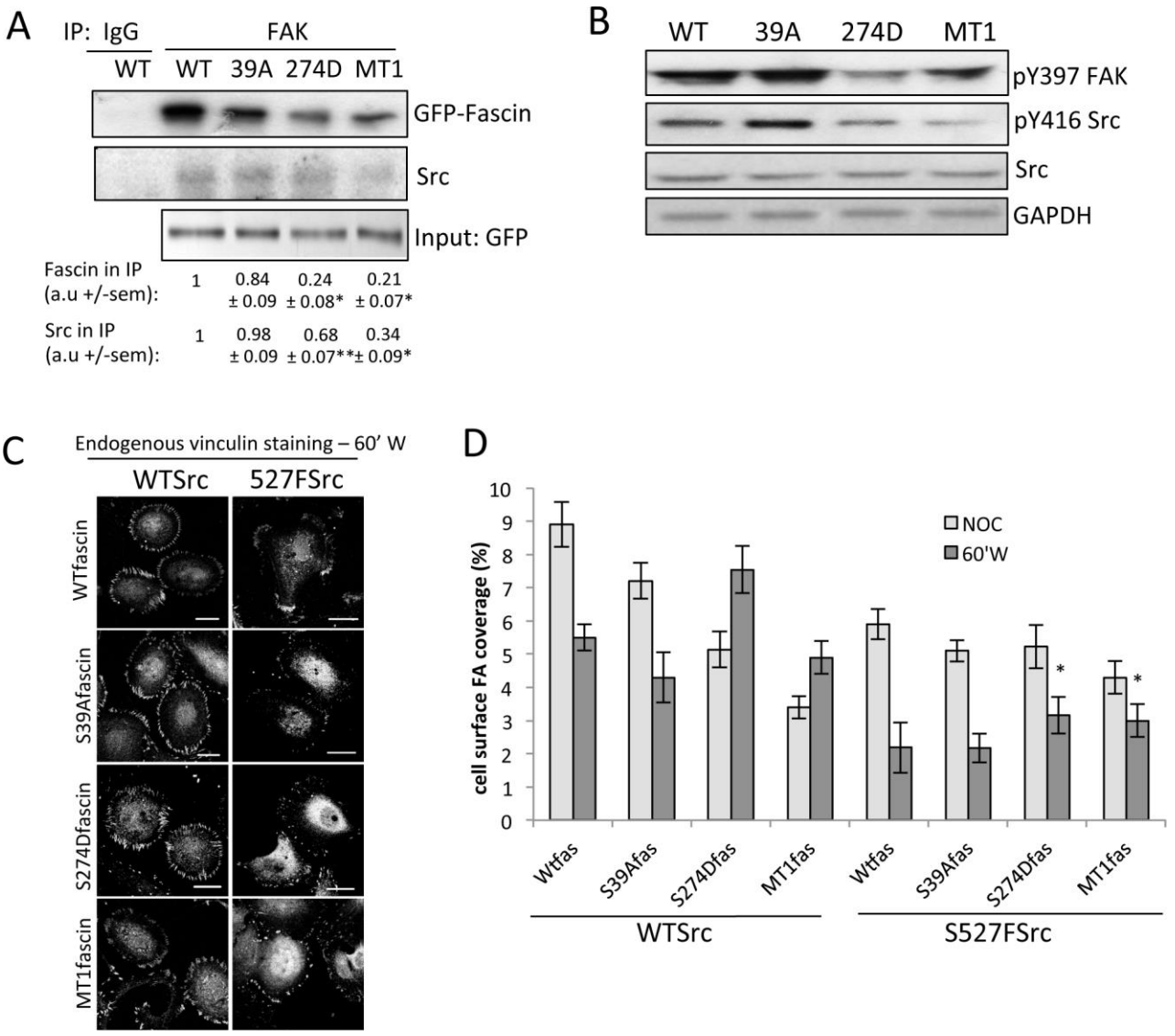


**Figure 6: Microtubule-dependent adhesion dynamics are regulated through a fascin-FAK-Src signaling pathway**

**(A)** Western blots of lysates from fascinKD cells expressing WT, S39A, S274D or MT1 fascin-GFP immunoprecipitated with control (IgG) or anti-FAK antibodies. Blots of IP's (left panel) were re-probed for specified proteins. Values are denoted below each respective lane and represent relative intensity of each band as a mean of the 4 experiments +/-SEM. *=p<0.001, **=p<0.05 compared to untreated controls. **(B)** Western blots of lysates from fascinKD cells expressing WT, S39A, S274D or MT1 fascin-GFP probed with specified antibodies. **(C)** Representative images of vinculin staining in fascinKD HeLa cells expressing WTSrc-GFP or constitutively active S527FSrc-GFP with WT, S39A or 274D-fascin-mFP 60 minutes post-NOC washout. Scale bars are 20 µm. **(D)** FA coverage per cell was quantified from cells treated with NOC for 20 minutes or following 60 minutes NOC washout. N=45 cells were quantified across 3 independent experiments. Mean values +/-SEM are shown, *=p<0.01 compared to WTfascin.

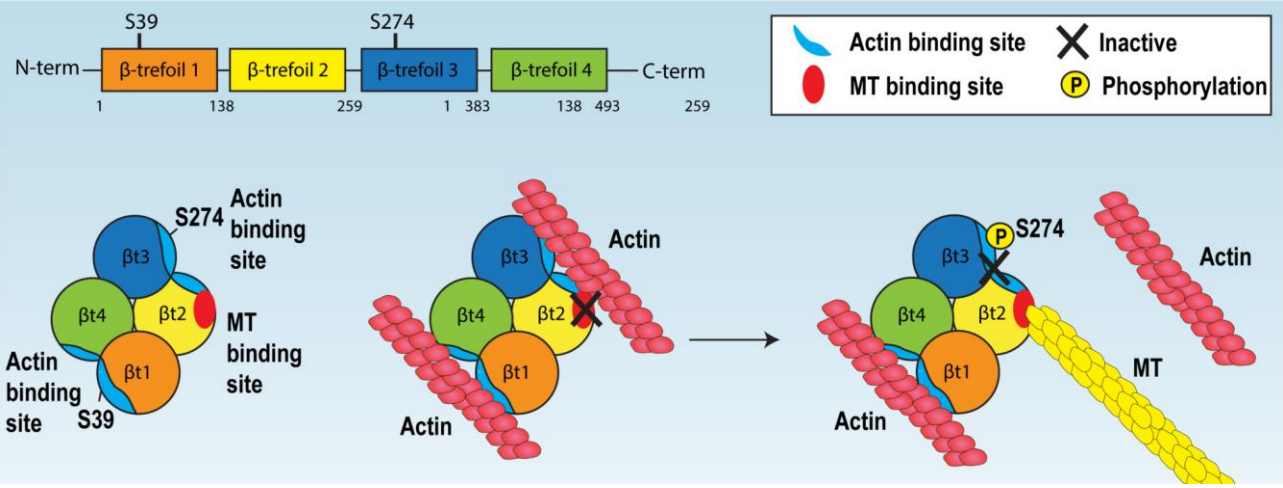


**Figure 7: Proposed model of fascin cytoskeletal associations**

Model for fascin-dependent association with F-actin or microtubules. See discussion text for details.